

Copper and mercury - microbiota

by Copper And Mercury Microbiota

Submission date: 08-Apr-2023 11:21PM (UTC+0500)

Submission ID: 2059104946

File name: Cu-Hg-Microbiota-Revision-I-SI.docx (1.7M)

Word count: 4628

Character count: 25884

1 Copper and mercury exposure alters rectum microbiota in female adult mice

2

3 Abstract

4 *Objectives:* ¹ Copper (Cu) and mercury (Hg) are major pollutants worldwide, but the
5 gastrointestinal damage caused by copper and mercury exposure is unclear. We are committed
6 to scientific research on the harm and transformation of copper and mercury exposure to the
7 rectal microbial population of female mice.

8 *Methods:* Kunming mice (n = 24) were randomly divided into four equal groups, i.e., 1) Rectal
9 Colon Control (RCK) group, 0 mg/kg of Cu and Hg), 2) Rectal Copper (RCu group), 5 mg/kg
10 weight of Cu), 3) Rectal Mercury (RHg) group, 2 mg/kg weight of Hg) and 4) Rectal copper-
11 mercury (RCH) group, 2.5 and 1 mg/kg weight of Cu and Hg. On the 90th day, the rectal and
12 intestinal tissues were analyzed for pathophysiology, and quantitative analysis by PCR, then a
13 library was prepared, and sequencing was carried out.

14 *Results:* The rectal tissue of the RCu and RCH group had histopathological and physiological
15 damage, including low weight, low pH value, increased thickness of the outer muscle layer,
16 smooth muscle tissue, widening of the submucosal layer, reduction of goblet cells, blunt
17 ² intestinal villi and severe aging of the central mammary duct. In addition, Sequencing results
18 of 16S rRNA genes compared with RCK showed that the abundance of the Treponema,
19 Coprococcus, and Dehalobacterium in RCu was more significant than the RCK. Still, the
20 bacillus, Jeotgalicoccus, Salinicoccus, Staphylococcus, and Ignatzschineria was just the
21 opposite. The abundance of Butyricimonas, Streptococcus, Dehalobacterium, Coprococcus,
22 Oscillospira, and Helicobacter in RHg was more significant than in the RCK. Still,
23 Corynebacterium, Bacillus, Jeotgalicoccus, Salinicoccus, Staphylococcus, Lactococcus, and
24 Ignatzschineria were the opposite. We found some similar exciting things. The abundance of
25 the Dehalobacterium, Coprococcus, and Oscillospira was significantly more significant than
26 the RCK. Still, the Corynebacterium, Salinicoccus, Jeotgalicoccus, Staphylococcus,
27 Lactococcus, Sutterella, and Ignatzschineria were the opposite. In addition, the Staphylococcus
28 in RCu was increased than in the RCH, and the Streptococcus in RCu was increased than in
29 the RCH.

30

31 *Conclusion:* The results of the present study ³ furnish a source for a more precise validation of
32 the risk of digestive tract diseases driven by Cu and Hg.

33

34 **Keywords:** Mice, Intestinal microbiota, Copper, Mercury, Rectum, 16S rRNA.

35 1. Introduction

36 Heavy metal pollution is a specific source of air pollution, such as environmental
37 pollution, mining, environmental quality, and animal concentrate (Zulkafflee et al., 2019).
38 Heavy metals such as copper and mercury are environmental pollutants causing health
39 problems for humans and other animals. Copper and mercury are two heavy metal
40 environmental pollutants. Copper is a key mining component and a common phenomenon
41 (Kim et al., 2000). On the other hand, essential minerals such as copper are nutrient elements
42 that can promote growth and development and assist in treating anemia. Still, it is also an
43 uncertain harmful substance, which depends on the amount of touch.

44 Mercury is a non-ferrous metal element but is also one of the heavy metals with the
45 highest toxic and side effects in the natural environment. Mercury is a toxic and harmful
46 pollutant, which is challenging to metabolize after entering the body and can harm fetal growth
47 beyond the embryo (Wang et al., 2017).

48 Many studies focus on transforming microbial strains and green plant rhizome groups
49 in areas polluted by copper and mercury (Uriu-Adams and Keen, 2005). Still, little attention
50 is paid to animals' physical and mental health. According to bioconcentration, because they
51 are also victims of copper and mercury pollution, animals have a similar system to adjust heavy
52 metals, namely intestinal microbiota. The intestinal microbiota is a wide variety of microbial
53 strains that settle on the length and total width of the digestive tract of lactating animals (Lee
54 and Hase, 2014). Today, the intestinal microbiota endangers the host organ/system and shows
55 everyone's interdependence and coevolution (Song et al., 2018). The uptake of copper and
56 mercury is carried out through the intestines and stomach. Therefore, copper and mercury
57 pollution will undoubtedly have a beneficial or harmful impact on intestinal microorganisms.
58 Some new information is likely to appear in transforming intestinal bacteria in animals polluted
59 by copper and mercury.

60 This experiment was studied to investigate the harm and transformation of copper and
61 mercury to the microbial population of mouse rectum. To achieve this better, we investigated
62 the composition of intestinal bacteria by evaluating the 16S rRNA transcriptome sequence.
63 Hopefully, results will help better understand the potential efficacy of copper and mercury in
64 gastrointestinal diseases.

65

66 2. Materials and Methods

67 *2.1. Compliance with Ethical Standards*

68 The Animal Health Care and Application Federation of Animal Science and
69 Technology, School of Jiangxi Agricultural University, approved all animal experiments.

71 *2.2. Samples Collection*

72 We have made every effort to minimize the pain of animals. All animals have obtained
73 the permission of the Animal Welfare Federation of Guangxi University. Twenty-four adult
74 female mice (7 days old; mean weight = 27.40 g) were randomly divided into four equal groups:
75 1) Rectal Colon Control (RCK) group, 0 mg/kg of Cu and Hg, 2) Rectal Copper (RCu group),
76 5 mg/kg weight of Cu), 3) Rectal Mercury (RHg) group, 2 mg/kg weight of Hg and 4) Rectal
77 copper-mercury (RCH) group, 2.5 and 1 mg/kg weight of Cu and Hg. Mice were trapped in
78 iron cages (n = 6/cage) and had access to a basic diet (Zhengzhou Tuduo Feed Technology Co.,
79 Ltd., Zhengzhou, Henan Province, China) and water *ad libitum*. This study used copper
80 chloride (CuCl₂) and mercury chloride (HgCl₂). On day 90, all mice were weighed and
81 euthanized before cervical dislocation. Colon contents from each mouse were harvested in an
82 Eppendorf tube (1.5 mL) under sterile conditions and stored at -80 °C for further analysis.

84 *2.3. Intestinal pathophysiological examination*

85 Morbid organs were collected for histopathology. The colon was dried, cleaned, and
86 placed in 10% neutral buffered formalin for fixation. Tissues were then washed, dehydrated
87 in ascending grades of alcohol, cleared in xylene, impregnated, and embedded in paraffin
88 tissues. Sections 4-5 μm thick were cut and stained with hematoxylin and eosin (Mujahid et
89 al., 2021). We examined tissue sections under a microscope (Zhao et al., 2020).

91 *2.4. DNA acquisition and amplification*

92 The total gene DNA of the mouse colon was obtained by Agilent high sensitive DNA
93 detection kit (Agilent, USA). Agilent 2100 (Agilent, USA) was used for DNA quantitative
94 analysis and detected DNA purity on 1 % agarose electrophoresis. We diluted the DNA with
95 diluent to 1 ng/mL with sterile water according to the concentration. The primers of 16S V4
96 were designed as 520f (5-aytggdytaaagng-3) and 802r (5-tacnvgggtatctacc-3). PCR Eppendorf
97 tube total volume was 50 μL composed of 25 μL Phusion composition of high-fidelity audio
98 PCR main mixture (New England Science Laboratory), 0.2 mm forward and reverse primer

99 design, and 10 ng DNA template. The RT-qPCR curve is as follows: 98 °C for 1min, 30
100 circulation systems at 98 °C for 10s, 50 °C for the 30s, and 72 °C for 60s.

101

102 2.5. *Quantitative evaluation and purification of PCR substances*

103 Mix the same volume of 1x loading buffer solution (Quant it PicoGreen dsDNA
104 analysis and detection kit, Invitrogen, file directory # p7589) with PCR substances. Then, we
105 tested it by electrophoresis on 1% agarose electrophoresis. We selected the samples with the
106 main band chromaticity in the middle of 400-450 base pairs for further testing. The PCR
107 materials were mixed with equal relative density and then purified with a genejet suspect gel
108 acquisition detection kit (Thermo Scientific). The increased substance was found on 1 %
109 agarose. According to the manufacturer's instructions, gelgreendna was used to color the
110 suspected glue in 1x Tris-acetate-EDTA (TAE) buffer solution. Then cleaned with wizard, SV
111 suspected glue, and PCR cleaning system software (Chambonel Les Promega in France).

112

113 2.5. *Library preparation and sequencing in advance*

114 Sequencing and analysis were carried out by M/S Parsonabio (Shanghai, China). In
115 short, according to the manufacturer's proposal, NEB NEXT1 ultratm DNA library applicable
116 to Illumina (Nebraska, USA) is applied to prepare the detection kit in advance, convert it into
117 a sequencing library, and add database index coding. Cupid dog evaluated the quality of the
118 library @ 2.0 fluorometer (Thermo Scientific) and Agilent 2100 system software (Agilent
119 2100). Finally, the library was sequenced on Illumina miseq service platform and transformed
120 into 250 bp /300 bp matched tail reading code.

121

122 2.6. *DNA-based data analysis*

123 Used Flash (V1.27) to splice paired tail reads from initial DNA fragments.
124 <http://ccb.kju.edu/software/flash>, the design scheme combines the pair's tail-end reading when
125 at least a part of the reading coincides with the task transformed from the other end of the same
126 DNA fragment. Assign matching end reading values to each sample according to the unique
127 barcode. Sequence analysis was carried out with uparse mobile phone software. Sequences
128 with 97 % homogeneity were assigned to consistent, practical operation classification modules
129 (OTUs). We selected a representative sequence for each OTU and annotated the classification
130 information network for each usual sequence using RDP support vector machine (Table 1).
131 According to the results of the OTU table, Chao1 index and Shannon index are calculated.

132 Originpro 8 data visualized the relative abundance of pathogen diversity patterns from door to
133 species.

134

135 2.7. *Measures of Microbial Diversity*

136 Alpha diversity analysis was carried out to assess whether the identified 16S rRNA
137 coding sequence contained all the bacteria in the sample. It was investigated using the
138 microbial strain biological quantitative analysis insight (QIIME) package (version 1.7.0). To
139 better evaluate alpha diversity, we used Chao 1 estimator and an ace to analyze community
140 richness and the Shannon index and Simpson index to analyze community diversity (Casquilho,
141 2016). The rarity curve illustrates that the total number of distinctive bacterial species is
142 challenging to increase with the increase of the number of identified coding sequences (Xu et
143 al., 2014). Unlike alpha diversity, beta diversity is a community structure used to study the
144 homogeneity between different samples scientifically. Total diversity (gamma diversity) is
145 determined by diversity at two levels: α Diversity and β Diversity. Principal component
146 analysis (PCA), multi-dimensional limit analysis (MDS), and cluster analysis were used to
147 consider sample differences. The detailed data has been submitted to NCBI short reading
148 archives database for query, and the login name is prjna418397.

149

150 2.8. *Statistical analysis*

151 Application SPSS19 0 for windows for statistical analysis. Nonparametric one-way
152 ANOVA, Mann Whitney U test, or trainee test was applied where appropriate. $P < 0.05$ was
153 considered statistically significant.

154

155 3. Results

156 3.1. *Body Weight*

157 The weight of mice in the copper test group (29.25 ± 0.25 g) was significantly lower
158 than that in the control group (31.49 ± 0.37 g). Compared with the RCK group, the colon of
159 the three treatment groups (RCU, RHg, and RCH groups) showed histopathological damage
160 (Fig. 1). The histopathological lesions comprised increased thickness of inner and outer
161 musculature, enlargement of the submucosa, mild to moderate necrosis of enterocytes, and
162 decreased number of goblet cells. There was slight to mild and moderate atrophy of intestinal
163 somatic cells, stunting and fusion of intestinal villi, and severe deterioration of the middle

164 mastoidal. Moreover, the length of the glands was significantly lower in the treatment groups
165 than in the control group.

166

167 3.2. *Beta Diversity Analysis*

168 The partial least squares discriminant analysis (PLS-DA) method is carried out on all
169 four groups (Fig. 2). The PLS-DA method is used to classify each group of samples, which
170 shows that people's classification method has a good performance.

171

172 3.3. *Sequence data and OTUs*

173 As shown in Fig. 3a, the OTUs were marked at the phylum to species and unclassified
174 by the RDP classifier, the 16S rRNA sequence, and the Green Gene database. The variations
175 of all 2912 were shown in the Venn diagrams Fig. 3b. A total of 1510 unique phylum OTUs
176 were presented in the Venn diagrams Fig. 3b. At the taxonomic genus level, 545 unique
177 bacterial genera were identified in all the samples. The OTUs (43.99 %) were highly similar
178 to the bacterial community structures, but each group had some unique OTUs. It can be seen
179 that unique OTUs in RCH, RCu, RHg, and RCH are 11.29, 0.66, 1.33, and 2.69 %, respectively.
180 This process demonstrated the distinctiveness, resemblance, and overlap of the OTUs
181 arrangement of the samples.

182

183 3.4. *Alpha Diversity of the Sequencing Data*

184 According to the sparse analysis of OTU, as shown in Figure 4 below, the recycled
185 sequence well represents the diversity of the four groups of bacterial biological communities.
186 The rarity curves of the observed species number (Fig. 4A), tide index value (Fig. 4b), and
187 Shannon index (Fig. 4C) achieve a service platform, depending on the identified sequence, is
188 likely to be enough to cover the bacteria in the sample plate. The level evolution rate curve
189 (Fig. 4D) and species accumulation curve are becoming more and more stable, indicating that
190 species are evenly distributed.

191

192 3.5. *The analysis is based on the phylum level*

193 As shown in Fig 5, 10 different doors are seen in the gastrointestinal contents.
194 Firmicutes, Proteobacteria, Bacteroidetes, and Acidobacteria exist in the bacterial community
195 as four significant dominant bacteria with an abundance ratio >1 visible. Among them,
196 Bacteroidetes and Firmicutes were the two most predominant bacterial groups. On the contrary,

197 the other 6 species were detected but showed lower relative abundance, composed of TM7,
198 Verrucomicrobia, Spirochaetes, Tenericutes, Deferribacteres, and Cyanobacteria. The
199 comparison of the homogeneity spacing of bacterial communities reveals some interesting
200 findings. However, the abundance of bacteria changed in the three groups but not significantly
201 relative to the RCK group, except for Spirochaetes.

202

203 3.6. *The analysis based on the genus level*

204 It can be seen from Fig. 6a that a total of above 20 genera are identified in samples and
205 composed of Allobaculum (11.26 ± 5.61 %), Lactobacillus (8.9 ± 4.34 %), Bifidobacterium
206 (8.17 ± 3.82 %), Bacteroides (3.95 ± 2.20 %), Staphylococcus (3.40 ± 5.83 %), Oscillospira
207 (2.87 ± 1.81 %), Adlercreutzia (1.37 ± 1.22 %), Sutterella (1.13 ± 0.99 %). And the low
208 abundance is composed of 39 species of other bacteria. However, in contrast to the smaller
209 changes in the phylum level, the abundance of bacteria dramatically changes at the genus level.
210 It can be seen from the graph the dominant genus had different abundances among the four
211 samples. There was a significant abundance of Treponema, Coprococcus, and,
212 Dehalobacterium in RCu compared to the RCK group. Still, the bacillus, Jeotgalicoccus,
213 Salinicoccus, Staphylococcus, and Ignatzschineria was just the opposite. The abundance of
214 Butyricimonas, Streptococcus, Dehalobacterium, Coprococcus, Oscillospira, and Helicobacter
215 in RHg was significantly larger than in the RCK group. Still, Corynebacterium, Bacillus,
216 Jeotgalicoccus, Salinicoccus, Staphylococcus, Lactococcus, and Ignatzschineria were the
217 opposite. And then, we can find some similar exciting things, the abundance of the
218 Dehalobacterium, Coprococcus, and Oscillospira was also obviously larger than the RCK, but
219 the Corynebacterium, Salinicoccus, Jeotgalicoccus, Salinicoccus, Staphylococcus,
220 Lactococcus, Sutterella and Ignatzschineria was just the opposite. In addition, the abundance
221 of Staphylococcus in RCu was larger than in the RCH, and the quantity of Streptococcus in
222 RCu was significantly larger than in the RCH.

223

224 4. Discussion

225 In humans, healthy gut microbiota plays a vital role in the host, giving kinetic energy,
226 nutrients, and immune maintenance (Safari and Younessi, 2017). In addition, it has certain
227 tolerance and some extreme standards that can change them, such as heavy metal pollution (Li
228 et al., 2019). Copper is an essential nutrient for all animals, and too much may lead to anorexia,
229 nausea, vomiting, always wanting to sleep, and gastrointestinal bleeding (Ding et al., 2019).

230 Mercury has strong toxic side effects in cell biology and physiology. Mercury in organic form
231 can cause corrosive esophagitis, intestinal bleeding, and GI tract diseases, such as corrosive
232 esophagitis and fecal bleeding. The damaged GI tract threatens the digestion and assimilation
233 of nutrients, resulting in weight loss (Wu et al., 2020). It is reported that excessive exposure
234 to copper will lead to the release of active substances of microbial strains, such as biological
235 macromolecular humic acid and acid-rich or microbial strain exudate (Ruan et al., 2019).
236 Water-soluble mercury salt is strong and highly toxic, which can cause general corrosive harm
237 to the gastrointestinal tract. In RCu and RHg groups, the thickness of adventitia, muscle fibers,
238 the submucosal layer, and the aging of intestinal villi increased significantly, indicating that
239 copper and mercury have damaged the intestinal tract of mice.

240

241 4.1. *Copper Effects on Intestinal Microbial Community*

242 In our study, compared with RCK, *Treponema*, *Coprococcus*, and *Dehalobacterium*,
243 the total number of dehalogenation bacteria in the colon of RCU patients increased significantly.
244 *Micrococcus* is a pathogenic bacterium that can cause diarrhea. Sueyoshi and Adachi (1990)
245 also found that gastrointestinal damage promotes the production of *Micrococcus* according to
246 the synergistic effect between gastrointestinal mucosal digestion and absorption injury,
247 metabolic improvement, and growing immature squamous epithelial cells. Dehalogenation
248 bacteria are Gram-positive bacteria with negative bacteria. Gram-positive and negative
249 bacteria have a unique intake system for inorganic copper on periplasmic protein (Trueba
250 Santiso et al., 2017). The resistance of inorganic copper is located on transposons, plasmids,
251 and bacterial sex chromosomes and is encoded by the gene of mer operon. However, the
252 protein MERP can transfer harmful positive ions to the mercury transporter *Mert* and transport
253 it to the nucleus to avoid the toxic effect of Gram-positive bacteria (Biondi et al., 2016). It
254 documented that the harm of copper environmental pollution to the growth and development
255 of Gram-negative bacteria is lower than that of Gram-positive bacteria (Khalid et al., 2021).
256 This is consistent with other researcher's results; that is, the evolution rate of Gram-negative
257 bacteria will be relatively increased, while the evolution rate of Gram-positive bacteria will be
258 reduced (Vincent et al., 2018). *Coprococcus* is the key cause of bacterial infection, but its
259 pathogenesis is unclear.

260 In contrast, *Bacillus*, worldwide bacteria, Gram-negative bacteria, *Staphylococcus*
261 *aureus*, and *Ignatzschineria* decreased significantly. Some reports indicate that *Bacillus*
262 microbial strains are part of traditional Chinese medicine preparations of compound probiotics,

263 such as *Bacillus subtilis* and *Bacillus licheniformis*. With the abundance of iodine ions,
264 galactosidase activity is inhibited, and the concentration of *Bacillus subtilis* decreases, which
265 may be a key reason for the decrease of *Bacillus subtilis*. β -Galactosidase can catalyze the
266 reaction of PG (nitrobenzene- β -D-galactopyranoside) reaction that hydrolyzes galactose and
267 nitrophenol (ONP) Streptococcus can cause.

268 In the absence of inducers, *Bacillus subtilis* (Warmerdam et al., 2013). It immediately
269 brought opportunities for the growth of bacteria. In the phylogenetic tree analysis of previous
270 scientific research, there are some similar characteristics between Jeotgalicoccus and
271 Salinicoccus (Papadioti et al., 2017). These two bacteria are regarded as potentially beneficial
272 for humans, producers, and operators. They may be one of the main functional groups of
273 intestinal microbiota and play a leading role in human health (Zhang et al., 2015). In addition,
274 it is reported that diffuse copper exposure can affect the composition of immunity-related fish
275 intestinal microbiota (Babcock et al., 2014). Therefore, reducing these bacteria may also
276 endanger the main role of all normal microbial populations in the colon, endanger colon
277 metabolism, and cause digestive and absorption nerve dysfunction. *Staphylococcus aureus* is
278 a Gram-positive bacterium belonging to the Staphylococcaceae family (Jin et al., 2020;
279 Bierowiec, 2020). Though *Staphylococcus aureus* is mostly copper-resistant due to metal
280 homeostasis and resistance systems (Al-Tameemi et al., 2021), very few reports indicate that
281 Gram-positive bacilli are likely to be endangered in the condition of copper environmental
282 pollution.

283

284 4.2. Mercury Effects on Intestinal Microbial Community

285 The Butyricimonas, Streptococcus, Dehalobacterium, Coprococcus, Oscillospira, and
286 Helicobacter in RHg significantly exceeded RCK, but the Corynebacterium, Bacillus,
287 Jeotgalicoccus, Salinicoccus, Staphylococcus, Lactococcus and Ignatzschineria was just the
288 opposite. The way bacteria resist heavy metals is different; Cu²⁺ is likely to accumulate
289 according to Cora-Mg²⁺ transporter. In addition, Cu²⁺ accumulates according to P-type
290 ATPase in the case of copper starvation (Lunin et al., 2006). The drug resistance system similar
291 to Pseudomonas cop system software is still unclear, but in Gram-positive bacteria, P-type
292 ATPase seems to detoxify copper according to emissions. Pseudomonas copper resistant
293 system software usually numbers four proteins, which fuse copper in the periplasm or near the
294 outer membrane. Hg²⁺ is converted into metallic mercury, spreading from somatic cells and
295 ring mirrors. Copper and positive mercury ions are important inflammatory factors.

296 The reduction of excessive heavy metal-oxygen ions will cause the formation of oxygen
297 free radicals. In addition, both copper and mercury decrease the body's content and activity of
298 superoxide dismutase (SOD) (Liu et al., 2019). These all lead to a reduction in oxygen. So,
299 we can see the increase of anaerobes, and the decrease of aerobic and facultative anaerobic in
300 our results, such as the increase of Treponema, Dehalobacteriaceae, Oscillospira, Helicobacter,
301 Streptococcus, Coprococcus, and Dehalobacteriaceae, while the decrease of Bacillus,
302 Staphylococcus, Salinicoccus, Ignatzschaineria, and Corynebacterium. Moreover, some
303 studies found that both copper and mercury can cause liver and kidney damage by lipid
304 peroxidation and immune injury, thus leading to low immunity (Aksu et al., 2017; Jurczuk et
305 al., 2004). At the same time, transforming the human immune system on the surface of the
306 mucous membrane is fundamental, especially the gene mutation of microbial population, which
307 may increase the number of pathogenic bacteria, such as Treponema and Butyricimonas, and
308 Helicobacter. It can also indirectly lead to decreased beneficial and harmless bacteria because
309 of the interaction between bacteria groups, such as Bacillus, Staphylococcus, and
310 Corynebacterium.

311 Some of the pesticides are copper based (Tegenaw et al., 2019) and usually lead to the
312 development of reactive oxygen species and free radicals (Kiaune and Singhasemanon, 2011);
313 in return, there is oxidative stress (Arnal et al., 2011). It has been documented that those
314 pesticides and their metabolites showed oxidative stress damage by inhibiting CAT and SOD
315 and increasing malondialdehyde (Wei et al., 2021). Catalase is an important antioxidant
316 enzyme that protects from oxidative stress and catalyzes hydrogen peroxide into water and
317 oxygen, consequently completing the detoxification process emulated by superoxide dismutase
318 (Li et al., 2022).

319 At the same time, some scientific researchers have found that excessive positive ions
320 of heavy metals produce side effects that are too dangerous for all physiological parameters,
321 including nitric oxide synthase (Gu et al., 2018; Chi et al., 2020). Even nutrient elements with
322 a good reputation, such as Zn²⁺, especially Cu²⁺, are harmful at higher concentrations. The
323 change of pH value greatly harms the growth and development of bacteria. In this study, we
324 found that the pH value of mice in the copper group was lower. These two aspects may also
325 be the primary reason for the transformation of beneficial bacteria.

326 4.3. *The Effects of Copper and Mercury on the Intestinal Microbial Community*

327 Interestingly, we found commonalities similar to the RCu and RHg groups at the
328 phylum, but some differences are. Copper is a sword with two edges, not only toxic but also

329 nutritious. There could be other reasons for increased Coprococcus, the only beneficial bacteria
330 in the RCu group. But mercury is ⁸ the heavy metal with the strongest toxicity, so the bacteria
331 change is larger than that of copper, no matter which way it is. In addition, gram-negative
332 bacteria are more resistant to metals than gram-positive bacteria (Safari and Younessi, 2017).
333 Thus, most of the mutant bacteria in our results were gram-positive bacteria. Lactococcus had
334 copper resistance but no resistance to mercury, so there was a change in the RHg group but no
335 in the RCu group. Bacillus is mostly soil organisms, some of which are used to produce
336 antibiotic substances and are not normal components of the local microflora, and their variation
337 is reasonable. OscilloSpira is related to ¹⁷ body weight and was found to increase in the intestines
338 of fasted animals. In our results, the weight of the RHg group was lower than that of other
339 groups. In addition, we also observed the transformation of other genera, including
340 Butyricimonas. However, this genus is rarely reported to be related to copper and mercury
341 poisoning in animal models.

342

343 5. Conclusion

344

345

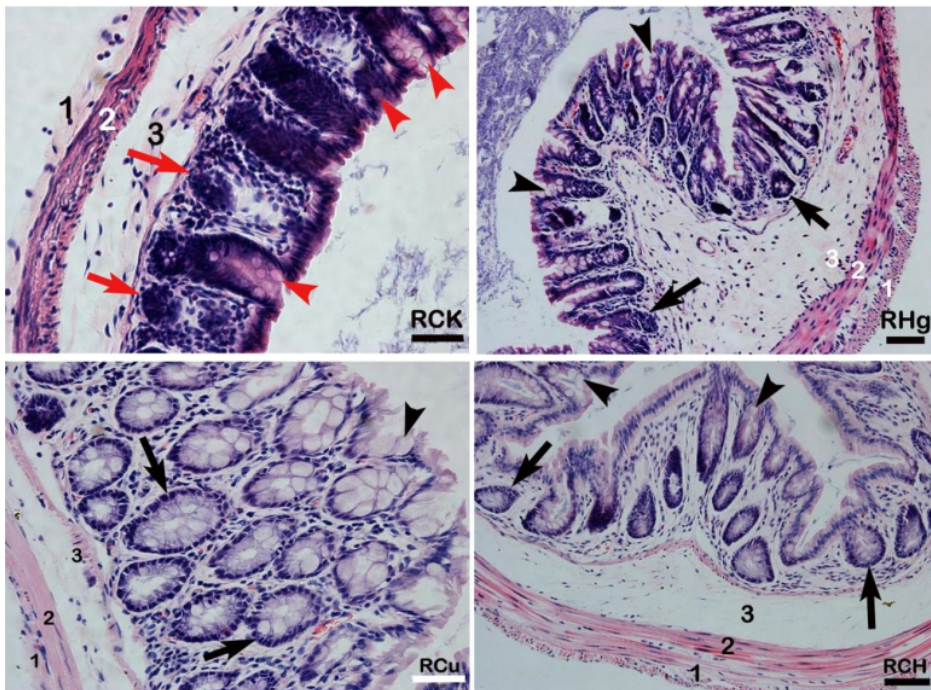
346 Overall, it is seen that high intakes of copper and mercury are likely to reduce the body weight
347 of mice. In addition, it also causes significant intestinal pathophysiological damage. The
348 histopathological lesions comprised of increased thickness of inner and outer musculature,
349 enlargement of the submucosa, and decreased number of goblet cells. There was slight to mild
350 and moderate atrophy of intestinal somatic cells, stunting and fusion of intestinal villi, and
351 severe deterioration of the middle mastoidal. Moreover, the length of the glands was
352 significantly lower in the treatment groups than in the control group. In addition, higher
353 concentrations of copper and mercury changed the diversity of the microbial population in the
354 whole process of female mouse attack, which may be the theoretical basis for describing the
355 poisoning system.

356

357 6. Novelty statement

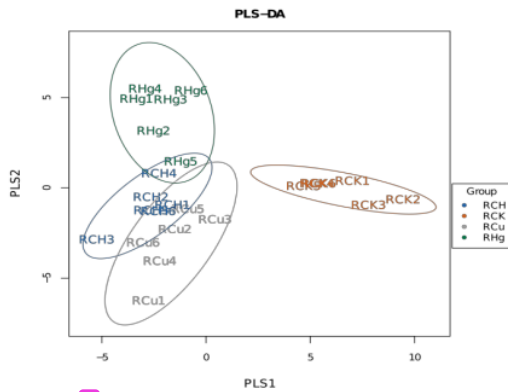
358 Normal rectum microbiota of various species has been studied extensively. Heavy
359 metals such as copper and mercury usually lead to pathological, hemato-biochemical, and
360 genotoxicity changes in humans and animals. However, scanty information about the effect of
361 copper and mercury on microbiota in the rectum is available, and this study has elucidated this
362 information.

363

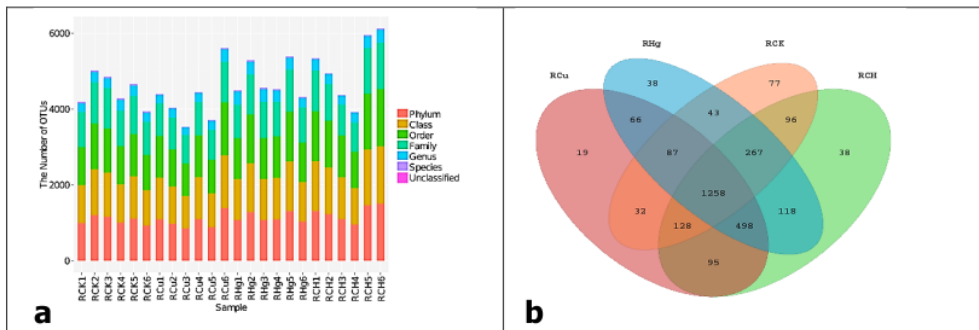


364

365 **Fig. 1.** Pathological analysis of colon mechanism. Control group (RCK group), copper
 366 group (RCu group), mercury group (RHg group), and copper-mercury group (RCH group).
 367 The numbers in the figure represent 1) the inner muscle layer, 2) the outer muscle layer, 3)
 368 the submucosal layer, goblet cells (arrowheads), intestinal glands (arrows), villi, and
 369 intermediate papillae. H & E, Bar = 20 μ m.
 370



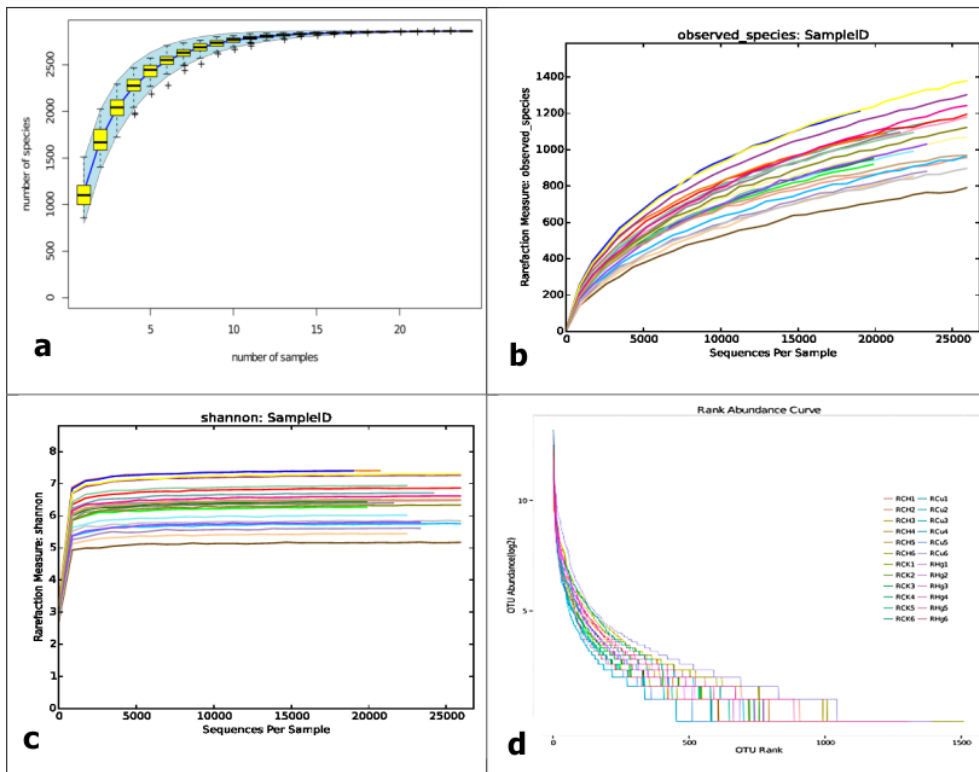
371 **Fig. 2.** Principal component analysis (PCA) of samples. The top 2 PCs are used as X and Y
 372 coordinates. Each sample represents a point. Samples from different sources have different
 373 colors: 1) RCH group (blue), 2) RCK group (orange), 3) RCu group (gray), and 4) RHg
 374 group (green).
 375
 376
 377



378 **Fig 3.** a) OTU identification and category data analysis results. OTU number of phyla, class,
 379 order, family, genus, and species. The number of OTUs that cannot be classified into all
 380 known groups is specified as "unclassified". b) The Venn diagram shows different groups'
 381 unique and shared OTUs.
 382

383

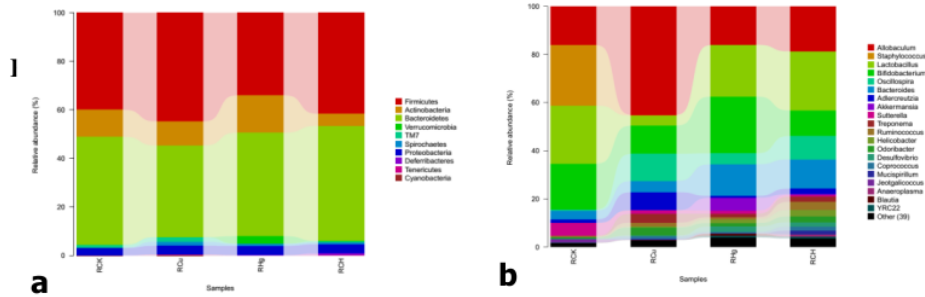
384



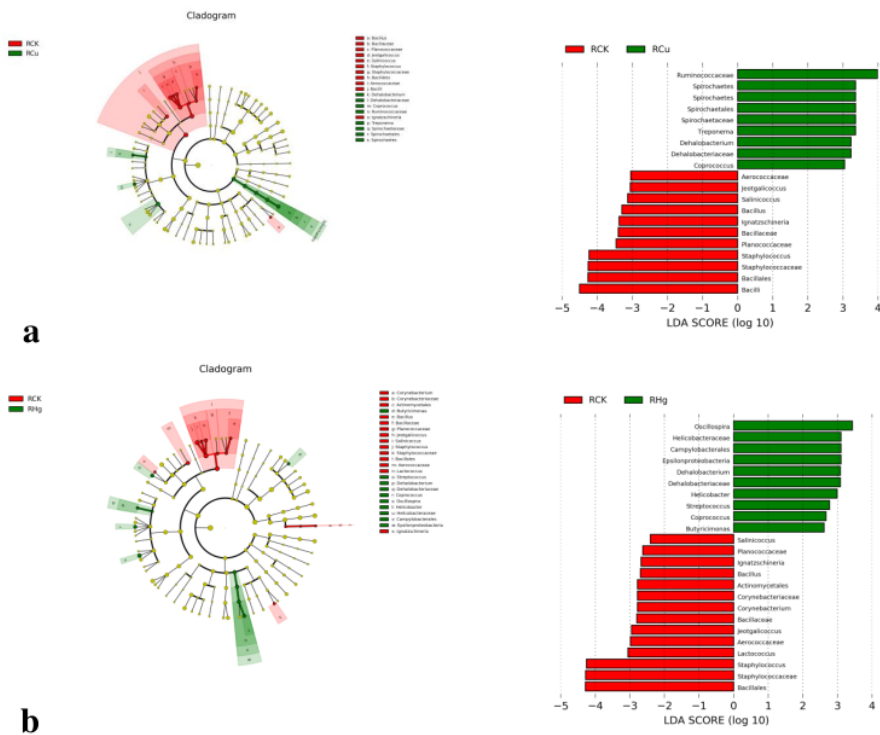
385

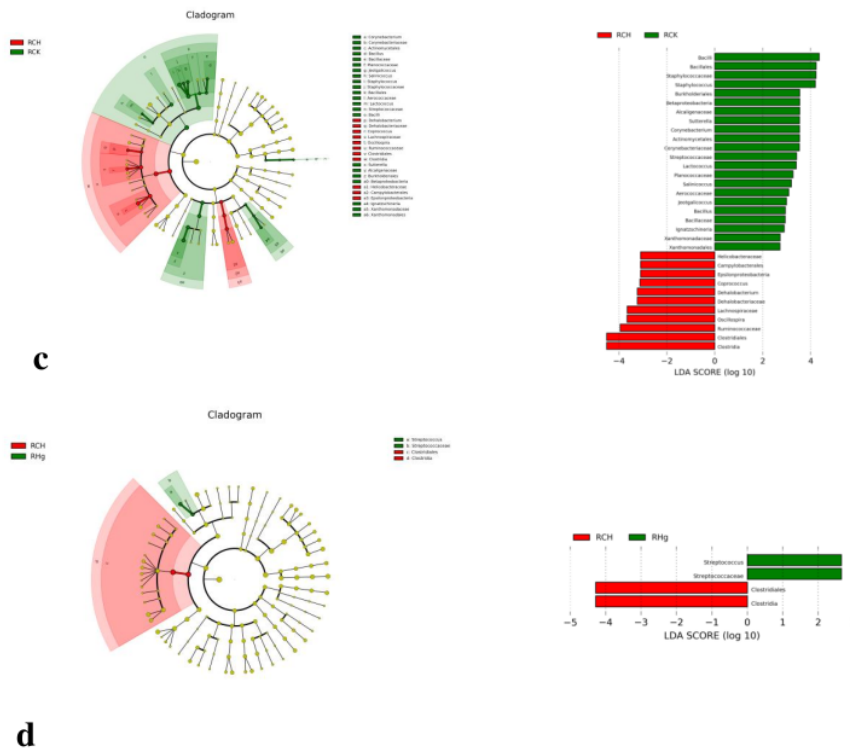
386 **Fig. 4.** a & b) Observe the rarity curve of alien species. c) Shannon curve. With the increase
 387 in identification sequences, the Shannon curve has become a service platform, which shows
 388 that the identification sequence can adequately cover the bacteria in the sample. d) Rank
 389 evolution rate curve. Each curve represents OTU distribution in one sample. The smoother
 390 the curve, the higher the symmetry of the plot.

391
 392
 393
 394
 395
 396
 397



398 **Fig. 5.** **a)** Relative abundances at the phylum level and **b)** Relative abundances under the
 399 bacterial genus.





400

401 **Fig. 6.** The branch diagram of significant differences between groups, including the
 402 comparison between the control group and RCU group (a), control group and rhG group (b),
 403 control group and RCH group (c) and its RCH group and rhG group (d). The branch diagram
 404 shows the level association of the template from door to genus (from inner ring line to outer
 405 ring line in the diagram). The size of the connection point indicates the mean relative
 406 abundance. The Yellow connecting point suggests that there is no significant difference
 407 between the two groups ($P > 0.05$), but other colors (such as emerald green and bright red)
 408 indicate that this OTU has a significant difference between the two groups ($P < 0.05$). LDA
 409 score means that there are different classification groups after copper or/and mercury solution
 410 (only classification groups conforming to $LDA \geq$ as shown in Figure 2.5 below).

411

412

413

414

415 ¹ **Table 1: Effective sequence and high-quality sequence**

Sample ID	Effective sequence	High quality	Ratio (%)	Sample ID	Effective sequence	High quality	Ratio (%)
RCK 1	28319	23714	83.74	RCU 1	51133	42394	82.91
RCK 2	35225	28821	81.82	RCU 2	27034	21757	80.48
RCK 3	30576	25357	82.93	RCU 3	27765	23100	83.20
RCK 4	70192	57896	82.48	RCU 4	29821	24024	80.56
RCK 5	28709	23319	81.23	RCU 5	29790	24590	82.54
RCK 6	27159	21454	78.99	RCU 6	78235	64589	82.56
RHG 1	52914	43455	82.12	RCH 1	48119	37368	77.66
RHG 2	37184	29415	79.11	RCH 2	27598	21376	77.45
RHG 3	46203	35738	77.35	RCH 3	28858	23049	79.87
RHG 4	54016	38715	71.67	RCH 4	28337	21360	75.38
RHG 5	50433	42046	83.37	RCH 5	51190	39552	77.27
RHG 6	29493	24516	83.12	RCH 6	46804	35999	76.91

416

417

418

Copper and mercury - microbiota

ORIGINALITY REPORT

15%

SIMILARITY INDEX

9%

INTERNET SOURCES

12%

PUBLICATIONS

%

STUDENT PAPERS

PRIMARY SOURCES

1

link.springer.com

Internet Source

5%

2

Sufang Cheng, Huirong Mao, Yezhao Ruan, Cong Wu, Zheng Xu, Guoliang Hu, Xiaoquan Guo, Caiying Zhang, Huabin Cao, Ping Liu. "Copper Changes Intestinal Microbiota of the Cecum and Rectum in Female Mice by 16S rRNA Gene Sequencing", Biological Trace Element Research, 2019

Publication

3%

3

Yezhao Ruan, Cong Wu, Xiaoquan Guo, Zheng Xu, Chenghong Xing, Huabin Cao, Caiying Zhang, Guoliang Hu, Ping Liu. "High Doses of Copper and Mercury Changed Cecal Microbiota in Female Mice", Biological Trace Element Research, 2018

Publication

1%

4

fridafashions.com

Internet Source

1%

5

Yuxuan Hong, Yingxian Cheng, Yanjuan Li, Xiaowen Li, Zutao Zhou, Deshi Shi, Zili Li,

1%

Yuncaï Xiao. " Preliminary Study on the Effect of TL on Cecal Bacterial Community Structure of Broiler Chickens ", BioMed Research International, 2019

Publication

6

www.researchgate.net

Internet Source

<1 %

7

Saranya Kizhakkilott Veedu, Gowthami Ayyasamy, Hema Tamilselvan, Mathan Ramesh. "Single and joint toxicity assessment of acetamiprid and thiamethoxam neonicotinoids pesticides on biochemical indices and antioxidant enzyme activities of a freshwater fish *Catla catla*", Comparative Biochemistry and Physiology Part C: Toxicology & Pharmacology, 2022

Publication

<1 %

8

D. H. Nies. "Microbial heavy-metal resistance", Applied Microbiology and Biotechnology, 1999

Publication

<1 %

9

"Bacteria in Agrobiolgy: Crop Productivity", Springer Nature, 2013

Publication

<1 %

10

www.mdpi.com

Internet Source

<1 %

11

farfar.pharmacy.bg.ac.rs

Internet Source

<1 %

12	www.duo.uio.no Internet Source	<1 %
13	Shi-quan Zhu, Jing Liu, Bo Han, Wen-peng Zhao, Bian-hua Zhou, Jing Zhao, Hong-wei Wang. "Fluoride exposure cause colon microbiota dysbiosis by destroyed microenvironment and disturbed antimicrobial peptides expression in colon", <i>Environmental Pollution</i> , 2022 Publication	<1 %
14	www.hindawi.com Internet Source	<1 %
15	www.researchsquare.com Internet Source	<1 %
16	peerj.com Internet Source	<1 %
17	bmcgastroenterol.biomedcentral.com Internet Source	<1 %
18	dx.doi.org Internet Source	<1 %
19	Jie Gong, Guoqing Shen, Mengru Zhu, Ming Zhan, Changjun Xi, Yan Shui, Zenghong Xu, Huaishun Shen. "16S rRNA gene sequencing analysis on changes in the intestinal flora of <i>Procambarus clarkii</i> with "Black May"	<1 %

disease", Journal of Oceanology and
Limnology, 2022

Publication

20

Lila O Vodkin, Anupama Khanna, Robin Shealy, Steven J Clough et al. "Microarrays for global expression constructed with a low redundancy set of 27,500 sequenced cDNAs representing an array of developmental stages and physiological conditions of the soybean plant", BMC Genomics, 2004

Publication

<1 %

21

apjr.net
Internet Source

<1 %

22

downloads.hindawi.com
Internet Source

<1 %

Exclude quotes Off

Exclude matches Off

Exclude bibliography On